energies

MDPI

Article

An Approach to Performing Stability Analysis for Power Transformer Differential Protection: A Case Study

Muhammad Sheryar [1], Muhammad Ahsan Ali [1], Farhana Umer [2], Zeeshan Rashid [2], Muhammad Amjad [3], Zunaib Maqsood Haider [2,*] and Muhammad Omer Khan [4]

[1] Department of Electrical Testing and Commissioning, Mansour Al Mosaid Group, Jeddah 22312, Saudi Arabia
[2] Department of Electrical Engineering, The Islamia University of Bahawalpur, Bahawalpur 63100, Pakistan
[3] Department of Electronics Engineering, The Islamia University of Bahawalpur, Bahawalpur 63100, Pakistan
[4] Department of Electrical Engineering & Technology, Riphah International University, Faisalabad 37000, Pakistan
* Correspondence: zunaib.haider@iub.edu.pk

Abstract: Differential protection normally detects short circuits and ground faults in the windings of a power transformer and its terminals. Inter-turn faults refer to flashovers among the electrodes that arise only in a similar type of physical winding. Inter-turn faults can be examined when the adequate sum of turns is served as short-circuited. In electrical protection, it is difficult to detect inter-turn faults. An inter-turn fault of small magnitude is based on the limited number of turns that resultantly provide a large quantity of current. Due to this reason, protection that comes from the differential scenario possesses a higher degree of sensitivity without causing unwanted operations during external faults. In this paper, a protection-based stability method is proposed whereby external voltages are applied at the low-voltage (LV) side of the transformer while keeping the high-voltage (HV) side short-circuited. This was conducted using a three-phase power transformer (rating: 100 MVA, 380 kV/13.8 kV) at SWCC Shoaiba Power Plant, Saudi Arabia. In this work, differential protection (87T) and high-impedance differential protection for HV-restricted earth faults (REFs) were verified by creating In-Zone and Out-Zone fault conditions to ensure current transformer (CT) circuits and tripping logic. All of the IEDs, protection, and control schemes involved were designed by ABB. This method verifies protection stability for power transformers by implementing differential protection (87T) and high-impedance restricted earth fault (64HV) schemes through creating In-Zone and Out-Zone fault conditions.

Keywords: power transformer; protection reliability; power transformer protection sensitivity; differential protection; external fault; CT saturation

Citation: Sheryar, M.; Ali, M.A.; Umer, F.; Rashid, Z.; Amjad, M.; Haider, Z.M.; Khan, M.O. An Approach to Performing Stability Analysis for Power Transformer Differential Protection: A Case Study. *Energies* **2022**, *15*, 9603. https://doi.org/10.3390/en15249603

Academic Editor: Pietro Romano

Received: 25 September 2022
Accepted: 18 November 2022
Published: 18 December 2022

1. Introduction

Electrical power transformers with a rating of more than 5 MVA have differential protection [1]. Compared with other protection strategies, transformer differential protection has significant benefits. A Buchholz relay can detect problems in the transformer that are located inside the insulating oil. However, if a fault develops in the transformer but not in the oil, it cannot be detected. Buchholz relays fall short of providing adequate protection against any bushing flash. These kinds of defects can be found using differential relays. Additionally, transformers have Buchholz relays to detect any internal faults; however, differential protection systems find these faults more efficiently. A differential relay analyzes the power transformer primary and secondary currents; if there is any imbalance, the relay activates and simultaneously trips the primary and secondary circuit breakers. The secondary windings of the CTs from the transformer's primary and secondary sides are connected in the opposite direction to the same-current coil of the differential relay so that there is no consequential current in that coil when the transformer operates normally. However, if a significant fault within the transformer disrupts the transformer's normal

ratio, the secondary current of both CTs does not remain the same, and a resultant current flows through the current coil of the differential relay, actuating the relay and tripping both the primary- and secondary-side circuit breakers. An appropriate examination of the conditions of a fault caused by the differential protection system must take into account voltage, current, and phase angle. The differential current remains zero for the normal load and external faults if the turn ratio and phase compensation are correctly designed. There are several reasons that cause unwanted differential currents, for instance, alteration in the tap-changer position, the features of loads, and transformer operating conditions. To make a differential relay as sensitive and stable as possible, restrained differential protection is developed for power transformers [2]. The restrained current or bias current provides restrictions for the differential relay operation. This stabilizes protection under fault conditions while still permitting the system to have good basic sensitivity. One way of defining the differential current (I_0) and bias current (I_b) [3] is by using Equations (1) and (2), where I_1 is the magnitude of the power transformer primary current and I_2 is the magnitude of the power transformer secondary current.

$$I_0 = I_1 - I_2 \tag{1}$$

$$I_b = \frac{I_1 + I_2}{2} \tag{2}$$

The transformer stability test is performed to ensure that the differential relay does not operate under normal conditions, even when load currents are high, and only operates when a fault occurs in its protection zone. The differential protection zone consists of a transformer and cables between current transformers. The cables are not covered when bushing current transformers (BCTs) are utilized [3].

2. Literature Review

The phase-locked loop technique developed in [1] gives a solution for converter-based distributed energy resources that trigger instability in smart transformers. A quartile-based differential protection method was designed to analyze the fault detection ratio of superimposed differential currents and was proved to be efficient in differentiating internal faults from other abnormal conditions [3]. Algorithms were specifically designed to maintain and improve the standard of performance of differential protection with the aim to reduce CT requirements and improve the period of grace in the case of CT saturation internal faults [4]. In 2013, an approach using the 3D current trajectory of transformer differential currents was developed for distinguishing between internal faults and in-rush currents [5]. The simulation of a transformer-biased differential protection scheme using MATLAB was conducted in a laboratory environment; the scheme was found to be efficient and reliable in solving differential relay issues such as tap changing, inherent phase shifts of currents in the transformer, CT ratios, and non-identical CTs [6]. An IEC-61850 sampled-values-based protocol for transformer differential protection was built; it transmits digitized values of currents and voltages on Ethernet frames and defines the testing procedure to test fault conditions, pickup, slope characteristics, and harmonic restraints [7]. In [8], the theoretical point of view associated with the testing of microprocessor-based quantitative protection relays was examined. However, the authors ignored the numerical testing of the double-phase pickup test and harmonic restraint as these are the major factors of differential protection relays [2]. An algorithm depending on the rate of increase in differential currents was developed in [9] for power transformer protection; it is able to distinguish between external disturbances (magnetic inrush) and the internal faults of the transformer. Digital differential protection for solid-state transformers using the ANSI-87T standard was developed in [10]. The authors employed high-frequency sub-band phenomena to detect internal faults using phase-let transform. The developed technique showcased improved performance in terms of accuracy, response time, and reliability during fault and normal operating conditions. The issue of detecting faults under CT saturation conditions was discussed in [11]. A stabilizing method was developed by the

authors using a combination of two signal processing indices to detect CT saturation. In [12], the authors discussed the issue of operational inaccuracy in substations having a one-and-a-half circuit breaker scheme. This issue arises when current is supplied to a transformer winding through a paralleling bay for its protection. The developed strategy demonstrated that external faults were desirably stabilized by the restraint current. The effects of integrating renewable energy resources in electrical power systems were discussed in [13], considering the detailed mathematical model of differential protection. An approach for detecting transformer faults using the Rogowski-coil-based model was developed in [14] to reduce the minimum operating point level and expand the protection zone of differential protection. An optimized hybrid approach was developed in [15] to improve the efficiency of a power transformer through the identification of suitable protection relays, and the online monitoring of loading conditions and inrush current of the differential relay. A space-vector-based technique was formulated in [16] to improve the sensitivity and accuracy of the differential protection of a power transformer by creating fault conditions such as over-excitation and inrush behavior. An effective testing method was proposed in [17] for the differential protection of three-phase power transformers considering zero, negative, and positive sequence currents. The proposed technique performed efficiently in stabilizing the symmetrical, asymmetrical, and external fault conditions. An approach for power transformer differential protection was presented in [18] considering the restrained and operating current values. The proposed strategy showcased efficient performance in harmonics and inrush scenarios. A mathematical model of digital differential protection was formulated using the wave-shape recognition method in [19]. The authors proposed a neural-network-based optimization algorithm to achieve stability during the internal and external fault conditions of a power transformer. In [20], a technique was presented, considering the symmetrical components of current, to detect CT saturation in digital relays. The effects of CT saturation were analyzed for different test conditions to make the differential protection of a power transformer more stable, sensitive, and reliable during normal operating conditions. The magnetizing currents play a crucial role in the operation of transformer differential protection [21]. To design sensitive differential protection, the detection of inrush current is very important [22]. A method based on phase angle variation was proposed in [23] to design effective differential protection. The proposed strategy can identify stable and fault limits using the waveforms of currents. In [24], the authors proposed an adaptive method to address the maloperation issue of transformers' differential protection owing to the magnetic saturation of current transformers (CTs). The effectiveness of the proposed strategy was demonstrated by comparing the results with those of conventional techniques. The authors developed an algorithm in [25] by employing the power–current scale to transform a differential protection. The proposed algorithm can classify the internal faults related to inrush behavior by analyzing the power and second harmonic current of a power transformer. A percentage bias differential scheme was proposed by the authors in [26]. The simulation results exhibit the efficacy of the proposed method against the internal phase and inter-turn faults of a power transformer. To minimize the difference in current for power transformer differential protection, a supervisory control and data acquisition (SCADA) system was developed in [27]. The simulation results prove the effectiveness of the designed scheme by detecting CT surplus current and protecting a transformer during fault conditions, in the minimum amount of time. To avoid CT saturation, the authors proposed an advanced differential protection methodology in [28] by considering the harmonics, geomagnetic disturbance conditions, and geomagnetically induced current.

3. Proposed Methodology for Differential Protection (87T)

The negative sequence differential protection (87T) is a very sensitive form of protection. It is used to identify internal faults such as turn-to-turn faults in a transformer winding. The protection relay "RET 670" is used in our case study. It has an "external/internal fault discriminator". In the case of a two-winding transformer, the external/internal fault dis-

criminator operation is based on the relative position of two phasors. In order to verify that a transformer differential protection relay is functioning accurately, and to ensure that all CTs' secondary circuits are correctly connected, a transformer stability test is performed [29]. This test is usually performed right before the energization of a power transformer, when the transformer itself and all the related electrical equipment (switchgear, CTs, PTs, power cables, relays, etc.) in the circuit are already tested and verified.

3.1. What Is a Stability Test?

The stability test is primarily performed to make sure that the CT selection and the setting parameters used for fault sensing are accurate. It indicates that sufficient current must be supplied to the CTs' primary HV and LV sides of a transformer in order to acquire a healthy reading on the CTs' secondary side to check the differential relay operation.

3.2. Different Methods to Perform Stability Test

Transformers place a high burden on a current source. At the site, the transformer HV-side differential CTs are mostly very far from the transformer LV-side CTs (connected via the MV/LV switchgear side). The distance between the HV-side and LV-side CTs can reach up to several miles depending upon the site design. Therefore, a current source is not feasible at the site. The more economical and safe way is to use an appropriate voltage source to supply sufficient current on CTs' primary side by shorting either side of a transformer winding. The shorting is applied after the CT that is used in the differential protection scheme. Usually, the voltage source is connected on the transformer HV side, and the transformer LV side is short-circuited. This method of testing is mainly used for stability tests. However, this test has some limitations in industries where the HV side of a transformer is connected to the gas-insulated switchgear (GIS) and applying an external voltage source to the HV side is not possible [30]. In this case, the voltage source is connected to the LV side and the HV side is short-circuited.

The proposed procedure to perform the transformer stability test using the differential protection technique for the 100 MV power transformer at the SWCC Shoaiba Power Plant, Saudi Arabia, is shown in Figure 1. In this method, external voltages are applied to the secondary side (LV side) of the power transformer using the generator and the primary (HV) side is kept short-circuited after differential CT [31]. The RET620 relay is used. This is a transformer management relay for the protection, control, measurement, and supervision of the process [32].

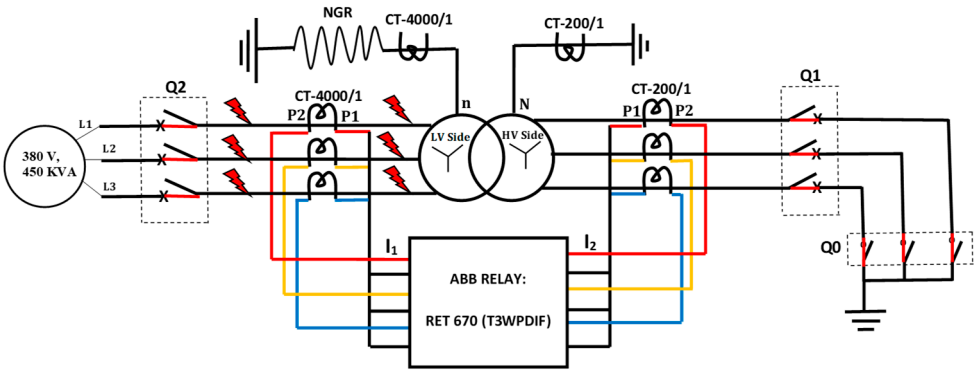

Figure 1. Proposed connection diagram for differential protection (87T).

The transformer vector group is YNyn0, with its HV side solidly grounded, and its LV side is grounded through a neutral grounding resistor (NGR). The HV and LV CTs have 200/1 and 4000/1 ratios, respectively. The HV and LV sides' neutral CT ratios are 200/1 and 4000/1, respectively. Q_0 is an earth switch, Q_1 is a primary side circuit breaker, and Q_2 is a secondary side switchgear circuit breaker. The power transformer technical details are mentioned in Table 1.

Table 1. Technical nameplate details for the power transformer at the Shoaiba site.

Parameter	Rating	Parameter	Rating
Rated Power (P_r)	100 MVA	Percentage Impedance (Z)	25.98%
CT Ratio (HV Side)	200/1 A	CT Ratio (LV Side)	4000/1 A
HV Rated Current (I_p)	151.9 A	LV Rated Current (I_s)	4183.7 A
Rated Voltage HV Side (V_p)	380 kV	Rated Voltage LV Side (V_s)	13.8 kV

The expected current generated during the stability test is calculated using Equation (3) [33]. Further calculations are performed as follows:

- Expected *LV*-side primary current, I_{LV} (Equation (4));
- Expected *HV*-side primary current, I_{HV} (Equation (5));
- Capacity of required voltage source, i.e., generator, S (Equation (6)).

$$\%\ Impedance\ (Z) = \frac{Rated\ Current \times Applied\ Voltage}{Rated\ Voltage \times Measured\ Current} \times 100 \tag{3}$$

At corresponding tap position of transformer

$$I_{LV} = \frac{V_{ext} \times I_s}{Z \times V_s} \times 100 \tag{4}$$

$$I_{HV} = \frac{V_s \times I_{LV}}{V_p} \tag{5}$$

$$S = \sqrt{3} \times I_{LV} \times V_{ext} \tag{6}$$

Here, V_{ext} is the applied test voltage, I_p is the transformer's rated primary current, I_s represents the transformer's rated secondary current, V_p is the transformer's rated primary voltage, V_s is the transformer's rated secondary voltage, Z is the percentage impedance, and S is the required generator capacity.

3.3. Expected Results and Calculations

The calculations are performed considering a 380 V generator as an external voltage source for *LV* winding, by keeping *HV* winding short-circuited, as described in Figure 1. I_1 and I_2 are the currents flowing through the *LV*- and *HV*-side CTs. Table 1 provides the values for V_{ext} = 380 V, I_p = 200 A, I_s = 4183.7 A, Z = 25.98%, V_s = 13,800 V, and V_p = 380,000 V. The results obtained using these values in Equations (1)–(6) are shown in Figure 2 for both stable and unstable conditions. A correction factor is employed for the secondary CT considering the primary CT owing to the different turn ratio of both CTs.

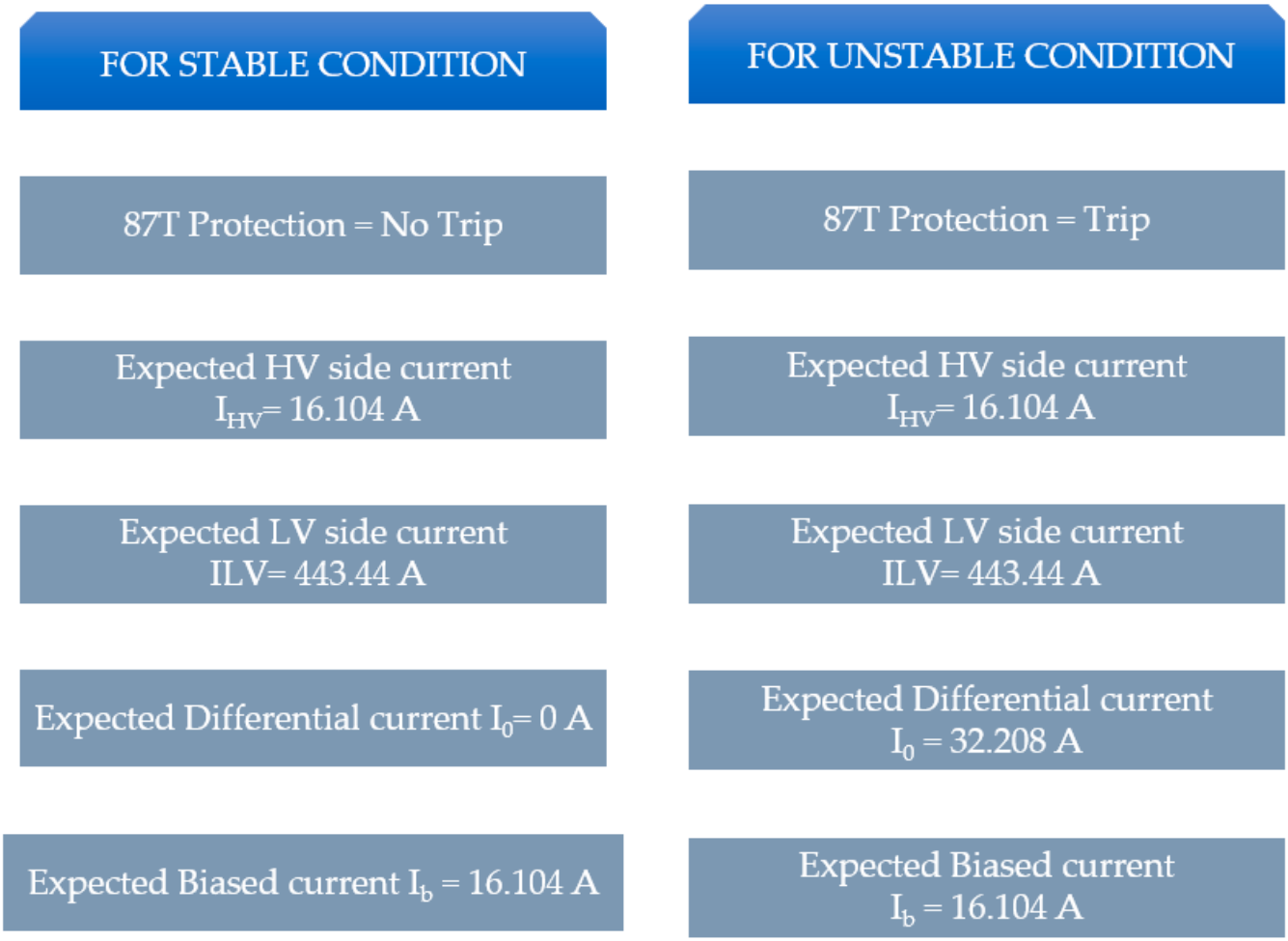

Figure 2. Expected results and relay operation for differential protection (87T) for the (**a**) stable condition and (**b**) unstable condition.

The third parameter is the required generator capacity. It is calculated by using Equation (6) to perform the test. The generator capacity should be at least 291.51 kVA. However, practically, most of the generators operate at nearly 70–80% of their capacity. Therefore, a generator of capacity 450kVA is used to perform the test. The technical details of the generator are given in Table 2.

Table 2. Technical nameplate details for the generator at the Shoaiba site.

Parameter	Rating	Parameter	Rating
Peak Rating (*S*)	450 kVA	Peak Rating (*P*)	360 kW
Amperes	650 A	Rated Output Voltage	380 V, 3 Phase
Power Factor	0.80	Frequency	60 Hz

4. Proposed Methodology for Single-Phase High-Impedance Restricted Earth Fault Protection (64HV)

Restricted earth fault (REF) protection is basically a form of differential protection. The only difference between differential protection and REF protection is that the latter is more sensitive compared with the former protection scheme. In the case of an internal fault for a single-phase high-impedance differential protection, the current cannot circulate and, therefore, is forced to flow through the measuring branch, triggering the relay to operate. For an internal fault, all involved CTs will try to feed the current through the measuring

branch. Depending on the fault current, relatively high voltages can be developed across the series resistor during the fault. To prevent the risk of flashover in the circuit, a voltage limiter must be included. The voltage limiter is a voltage-dependent resistor and is referred to as Metrosil (MS). A higher resistance value gives a higher sensitivity and vice versa [15]. The low-impedance restricted ground fault protection HZPDIF (87N) of ABB relay model RET670 is used at the site. It is a winding protection relay, as shown in Figure 3. It protects the power transformer winding against faults involving the ground. SR and MS in Figure 3 are the series resistor and Metrosil, respectively. To verify the stable and unstable conditions for 64HV, the switching operations are carried out as shown in Figure 4. NGR is bypassed to earth to avoid power dissipation. For Q_0, Q_1, and Q_2, only one phase L_1 is closed, and the current flows through L_1 under normal operating conditions.

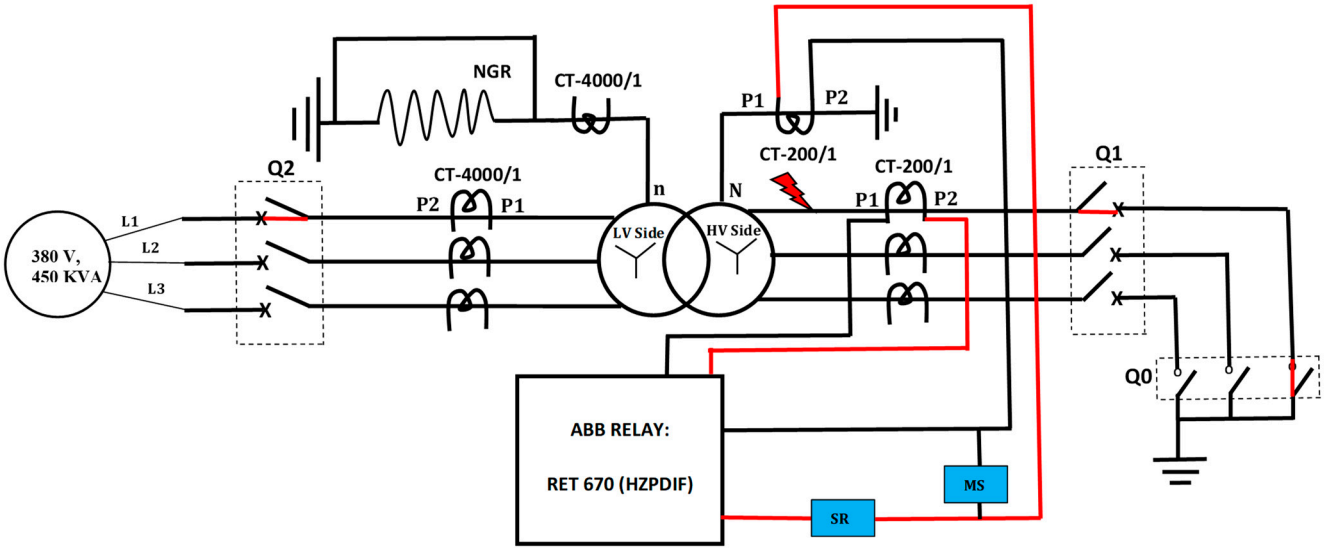

Figure 3. Proposed connection diagram for single-phase high-impedance differential protection.

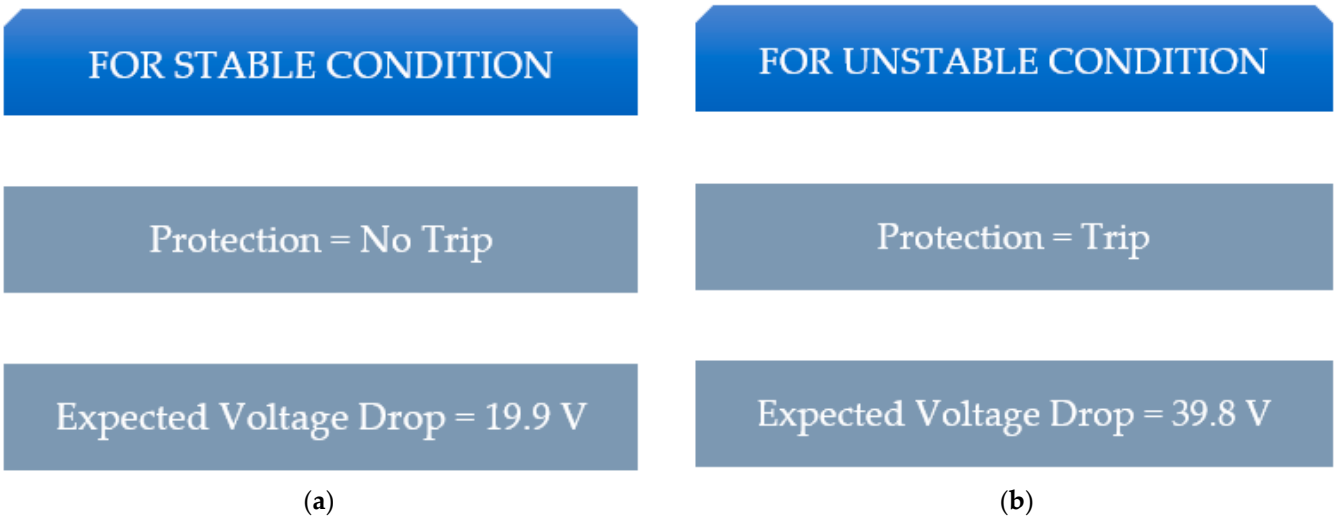

(**a**) (**b**)

Figure 4. Expected results and relay operation for single-phase high-impedance differential protection for the (**a**) stable condition and (**b**) unstable condition.

4.1. Calculations

The whole scheme, its components, and its wiring must be designed properly to withstand the abrupt change in voltage during an internal fault. Otherwise, any flashover in the CT secondary circuits or any other part of the scheme can cause the maloperation

of the high-impedance differential relay for an actual internal fault. The details of the site parameters for the calculation of single-phase high-impedance differential protection are given in Table 3.

Table 3. Parameter details for single-phase high-impedance differential protection.

Parameter	Value	Parameter	Value
CT resistance (R_{CT})	2 Ω	CT knee point (V_K)	400 V
CT cable lead resistance per meter (R_L)	0.0054275 Ω/m	Maximum CT lead cable length (N)	420 m

The maximum through fault current (I_f) is calculated by using Equation (7) based on the power transformer technical details, which are mentioned in Table 1.

$$P_r = 25\% \times \sqrt{3} \times V_p \times I_f I_f = \frac{100000 \text{ kVA}}{0.25 \times 1.732 \times 380 \text{ kV}} = 608 \text{ A} \quad (7)$$

I_f is the current at the primary side of the HV CT. Therefore, it needs to be referred to the secondary side of the *HV* CT:

Expected HV side secondary current $= 608 \times \frac{1}{200} \text{A} = 3.04 \text{ A}$, where 200/1 is the CT ratio of HV-side neutral CT.

The setting of the RET670 relay should be such that the relay must be stable for the maximum through fault current (I_f). We calculated the voltage developed across the relay (V_s) when a through fault occurs and one of the CTs goes into complete saturation. The value is calculated by using Equation (8), considering the data from Table 3.

$$V_s = I_f \times (R_{CT} + 2 \times N \times R_L) = 3.04 \times (2 + 2 \times 420 \times 0.0054275) = 19.9 \text{ V} \quad (8)$$

4.2. Expected Results

The 19.9 V is doubled during a ground fault, owing to the principle of differential protection. Therefore, the expected results and the protection operation for the stable and unstable conditions are summarized in Figure 4.

5. Results

5.1. Stability Test Results for Differential Protection (87T)

To perform a stability test for the transformer differential protection based on Figure 1, switching operations are performed in a sequence, which includes closing the earthing switch (Q_0) first and then the circuit breaker Q_1. The Q_2 circuit breaker is closed after verifying the generator voltage (380 V) and shorting all the phases of the HV side. In the first condition, the fault is between the secondary CT and the circuit breaker Q_2, as shown in Figure 1. This area is not covered by the differential protection. Therefore, the fault is out of the zone for 87T and there is no tripping operation performed by the relay, because the current magnitudes and the phase angles are normal, and a phase difference of approximately 180° is noted between the primary and secondary currents. The measurements taken from the display unit of relay RET670 are shown in Figure 5.

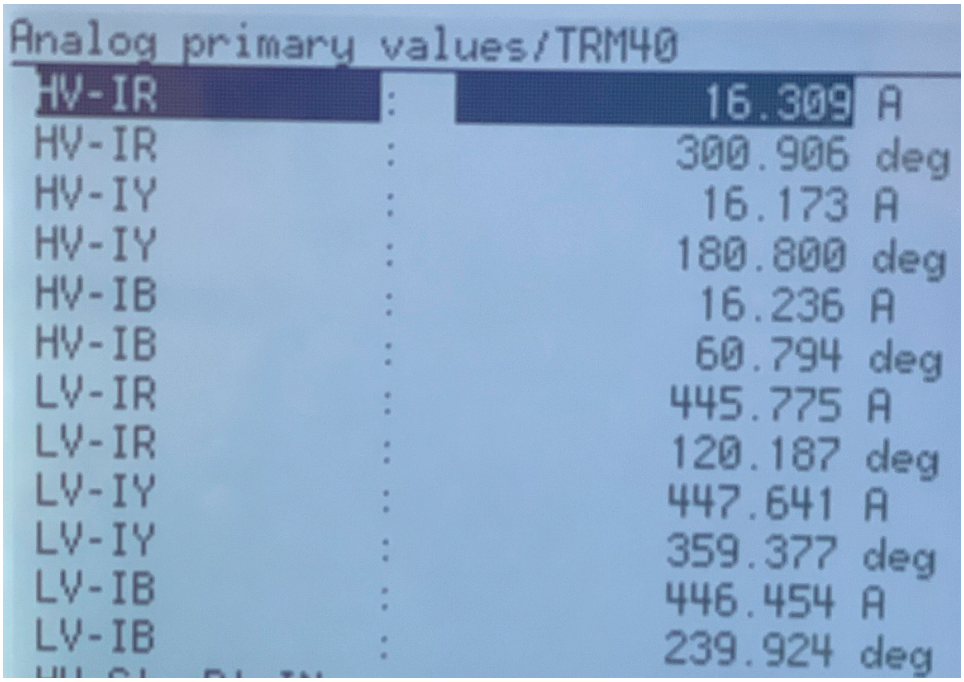

Figure 5. Measured values for HV and LV currents by the relay RET670 display unit [16].

Here, HV-IR, HV-IY, and HV-IB are the HV-side current measurements, and LV-IR, LV-IY, and LV IB are the current measurements at the LV side. The current measurements for both primary and secondary sides are almost equal to the expected current values, as calculated in Figure 2 for stable conditions.

At this time, the measured values of differential and biased currents by the relay are shown in Figure 6. It can be seen that the differential currents are almost equal to zero for all phases, and the measured values of biased and differential currents are the same as expected in Figure 2.

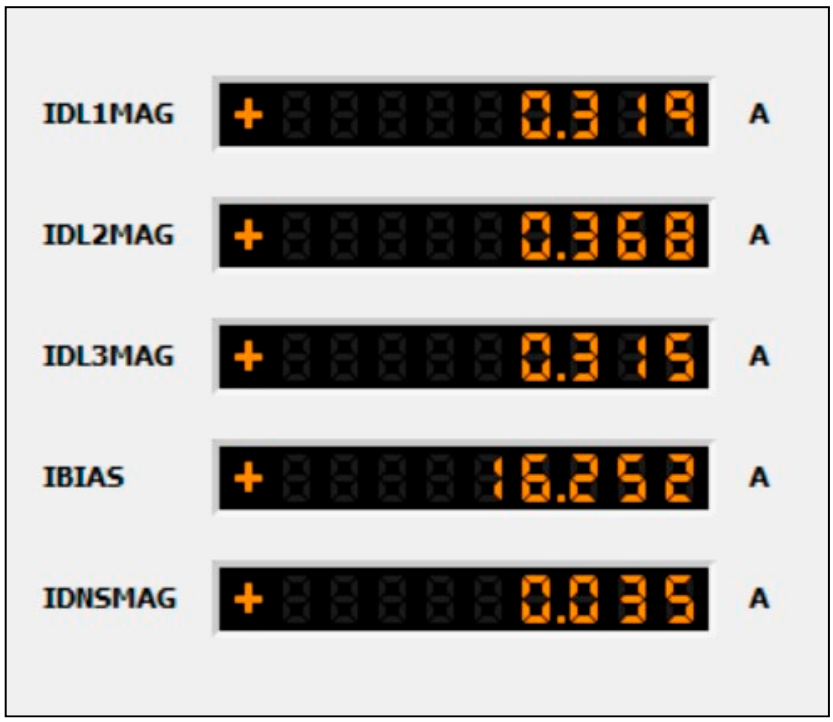

Figure 6. Measured values for differential (I_0) and biased (I_b) currents by the relay RET670 [16].

Here, IDL1MAG, IDL2MAG, and IDL3MAG are the values of differential currents for each phase. IBIAS is the value of the biased current. The protection operation is verified by the relay configuration software PCM 600, and the logic screenshot is shown in Figure 7. The T3WPDIF represents the differential protection block in the relay; the parameter T3WPDIF-TRIP output shows that the function is false, and the relay is in stable condition.

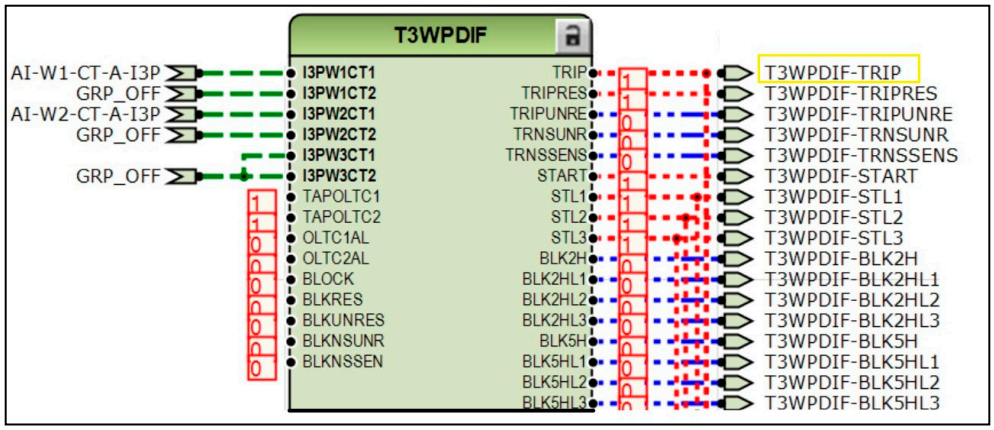

Figure 7. Measured protection operation by relay logic software ABB-PCM 600 [17].

5.1.1. Sensitivity Test Results for Differential Protection (87T)

To verify the sensitivity, the In-Zone fault is created at the *LV* side as shown in Figure 1, between the secondary-side CT and the *LV* side of the transformer, by swapping CT wires for *LV* phases towards the relay. In this condition, a differential current I_0 is measured through the relay for all phases, which is an unstable condition for 87T protection. It is verified that the differential protection is operated and both circuit breakers, Q_1 and Q_2, are tripped. The measurements taken from the display unit of the relay RET670 are shown in Figure 8.

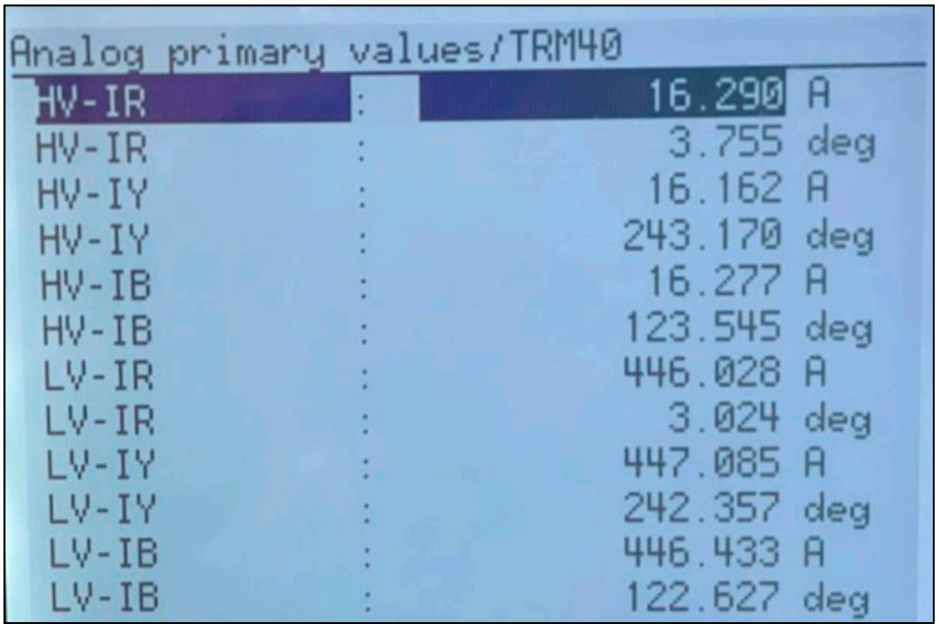

Figure 8. Measured values for *HV* and *LV* currents by the relay RET670 display unit [16].

These current values are the same as those shown in Figure 2. In Figure 8, it can be seen that the phase angle difference between the primary and secondary side currents is zero, which creates an unstable condition for differential protection. At this time, the

measured values of the differential and biased currents by the relay are shown in Figure 9. As the fault is In-Zone, it causes differential currents to flow through the relay. In all three phases, measured differential currents and the values of measured biased currents are the same as those shown in Figure 2.

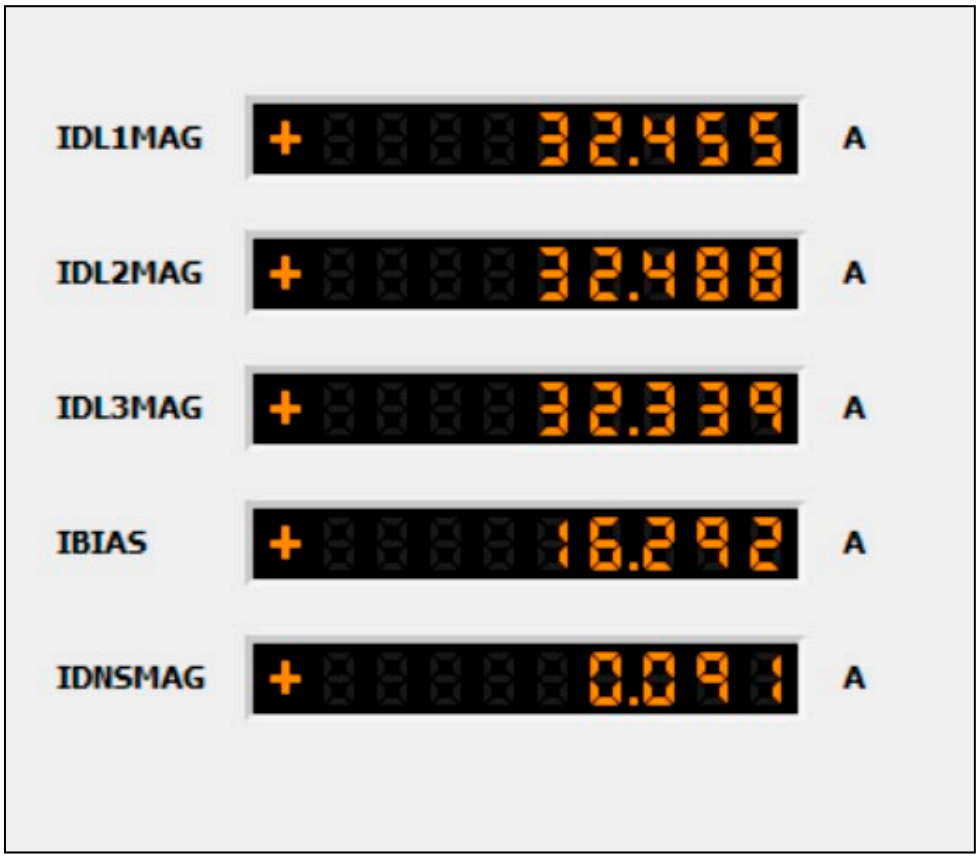

Figure 9. Measured values for differential (I_0) and biased (I_b) currents by the relay RET670 [16].

The protection operation is verified by the relay configuration software PCM 600. As shown in Figure 7, the protection function T3WPDIF is enabled, and the output parameter T3WPDIF-TRIP is true, which further causes the operation of the relay to trip breakers.

5.1.2. Comparison between Expected and Measured Values for Differential Protection (87T)

A comparison is drawn between the measured and expected results in Tables 4 and 5 to showcase the efficiency of the proposed method by verifying the sensitivity of transformer differential protection.

Table 4. Results comparison for the stable condition.

Expected Differential (A)	Average Measured Differential (A)	Expected Biased (A)	Measured Biased (A)
0	0.334	16.104	16.252
Expected Relay Operation		**Measured Relay Operation**	
No Trip		No Trip	

Table 5. Results comparison for the unstable condition.

Expected Differential (A)	Average Measured Differential (A)	Expected Biased (A)	Measured Biased (A)
32.208	32.427	16.104	16.292
Expected Relay Operation		**Measured Relay Operation**	
Trip		Trip	

5.2. Stability Test for Single-Phase High-Impedance Restricted Earth Fault Protection (64HV)

Based on Figure 3, a single-phase voltage is applied on the L1 phase only and no fault is created under this condition. The value of measured voltage by relay logic is shown in Figure 10. It is clear that the relay is in the normal condition, and there is no tripping. The measured voltage is found to be the same as that shown in Figure 4.

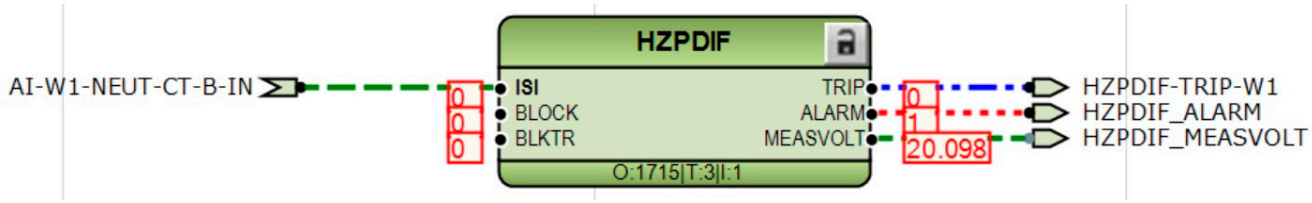

Figure 10. Measured protection operation and voltage by relay logic software ABB-PCM 600 after the stability test.

Here, HZPDIF-TRIP-W1 is a protection parameter that shows whether the protection is enabled or disabled, and HZPDIF_MEASVOLT is an analog parameter that gives the value of the voltage drop.

5.2.1. Sensitivity Test Results for Single-Phase High-Impedance Restricted Earth Fault Protection (64HV)

After verifying the stable condition, a fault is created at the L1 phase, between the HV-side CT and the transformer, by swapping the CT wires for HV-neutral CT, as shown in Figure 3. The values of measured voltage and relay operation are shown in Figure 11. The measured voltage is now double due to the unstable condition and the protection function is operated.

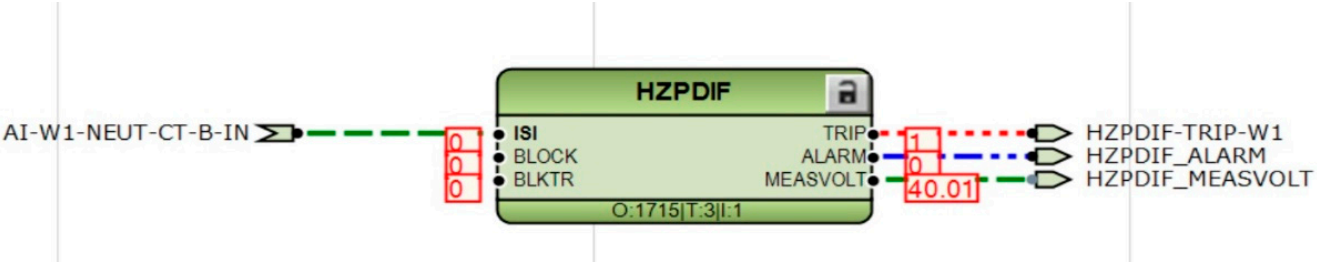

Figure 11. Measured protection operation and voltage by relay logic software ABB-PCM 600 after the sensitivity test.

5.2.2. Comparison between Expected and Measured Values for Differential Protection (87T)

A comparison is drawn between the measured and expected results in Tables 6 and 7 to prove the efficiency of the proposed method by verifying the sensitivity of transformer differential protection.

Table 6. Results comparison for the stable condition.

Expected Voltage Drop (V)	Measured Voltage Drop (V)	Expected Relay Operation	Measured Relay Operation
19.9	20.098	No Trip	No Trip

Table 7. Results comparison for the unstable condition.

Expected Voltage Drop (V)	Measured Voltage Drop (V)	Expected Relay Operation	Measured Relay Operation
39.8	40.01	Trip	Trip

6. Site Pictures

Some pictures of the site, such as of the power transformer, testing equipment, and protection relay while conducting the case study, are shown in Figure 12.

Figure 12. *Cont.*

Figure 12. Site pictures taken during the case study.

7. Conclusions

In this paper, a model is designed and practically verified for the stability of a power transformer using the differential protection principle. An approach is designed to evaluate the sensitivity of power transformer differential protection. To measure the magnitude of currents for HV and LV CTs, the external voltages (380 V) were supplied at the LV side of a power transformer by keeping the HV side ground, because if the voltage is applied to the HV side, there is a chance that a current of high magnitude will develop at the LV side. To verify operation, In-Zone and Out-Zone faults are first created according to the differential protection (87T) anticipated calculations.

Similar calculations and procedures were used to prevent HV REF. To enhance the sensitivity, the HV REF protection mechanism is voltage-operated. In order to assess the voltage drop across the resistor during a fault and to provide voltage measurements to the relay, a series resistor (SR) was utilized before the relay. The Metrosil was connected in parallel to protect the relay from high-voltage surges and fluctuations. To prevent tripping for through fault scenarios, the proposed method is effective at determining In-Zone and Out-Zone boundaries. This procedure can be used to verify the CT healthiness, coordination, and tripping operations of protection relays. The proposed approach is effective and is unaffected by the protection settings and CT ratios. The experimental results demonstrate that the proposed approach is efficient in identifying the external fault and transformer issues. Therefore, the proposed approach can be applied to applications where transformer stability is of considerable significance. Moreover, the designed procedure has proved to be the most effective method to perform transformer stability tests. It addresses the responsibility of the control engineers who investigate the design phase, testing, and commissioning of the pre-engineering activities. In our future work, the proposed approach will be extended to achieve maximum efficiency control for the protection relays by considering different loss components.

Author Contributions: Conceptualization, M.S., M.A.A., F.U., Z.R., M.A., Z.M.H. and M.O.K.; Formal analysis, M.S., M.A.A., Z.R. and Z.M.H.; Methodology, M.S., F.U., M.A., Z.M.H. and M.O.K.; Writing—original draft, M.S. and Z.R.; Writing—review and editing, F.U., Z.R., M.A. and M.O.K. All authors have read and agreed to the published version of the manuscript.

Funding: This research work was supported by the Office of Research Innovation and Commercialization (ORIC), The Islamia University of Bahawalpur, Pakistan (No. 3900/ORIC/IUB/2021).

Data Availability Statement: Not applicable.

Acknowledgments: We are very grateful to the Mansour Al Mosaid Group, Jeddah, Saudi Arabia, and the Office of Research Innovation and Commercialization (ORIC), the Islamia University of Bahawalpur, Pakistan (No. 3900/ORIC/IUB/2021), for providing the state-of-the-art platform required for measurements.

Conflicts of Interest: The authors declare no conflict of interest.

Nomenclature

The following acronyms, nomenclature, and constants are used in this manuscript:

REF	Restricted earth fault
CT	Current transformer
BCT	Bushing current transformer
SCADA	Supervisory control and data acquisition
PT	Potential transformer
LV	Low voltage
MV	Medium voltage
HV	High voltage
GIS	Gas-insulated switchgear
SR	Series resistor
Constants and Variables	
I_0	Differential current
I_b	Bias current
I_1	Primary current of power transformer
I_2	Secondary current of power transformer
I_{HV}	Current at high voltage side
I_{LV}	Current at low voltage side
V_{ext}	Applied test voltage
S	Generator capacity
Z	Percentage impedance
R_{CT}	Resistance of CT
V_k	Knee point voltage of CT
R_L	Lead resistance
I_f	Fault current
N	CT lead cable length

References

1. *IEEE Std C37.91-2021 (Revision of IEEE Std C37.91-2008)*; IEEE Guide for Protecting Power Transformers. IEEE: Piscataway, NJ, USA, 2021; pp. 1–160. [CrossRef]
2. Verzosa, Q.; Lee, W.A. Testing microprocessor-based numerical transformer differential protection. *IEEE Trans. Ind. Appl.* **2017**, *53*, 56–64. [CrossRef]
3. Zou, Z.; Liserre, M.; Wang, Z.; Cheng, M. Modeling and stability analysis of a smart transformer-fed grid. *IEEE Access* **2020**, *8*, 91876–91885. [CrossRef]
4. Shah, A.M. Quartile based differential protection of power transformer. *IEEE Trans. Power Deliv.* **2020**, *35*, 2447–2458. [CrossRef]
5. Moscoso, M.; Lloyd, G.J.; Liu, K.; Wang, Z. Improvements to transformer differential protection-Design and test experience. In Proceedings of the 47th International Universities Power Engineering Conference (UPEC) 2012, London, UK, 4 September 2012; pp. 1–6. [CrossRef]
6. Pires, V.F.; Cabral, A.; Guerreiro, M. Transformer differential protection based on the 3D current trajectory mass center. In Proceedings of the 4th International Conference on Power Engineering, Energy and Electrical Drives, Istanbul, Turkey, 13–17 May 2013; pp. 52–57. [CrossRef]
7. Upadhayaya, P.N.; Makwana, V. Modelling & simulation of transformer biased differential protection scheme in laboratory environment. In Proceedings of the International Conference on Intelligent Computing, Instrumentation and Control Technologies (ICICICT) 2017, Kannur, India, 6–7 July 2017; pp. 68–73. [CrossRef]
8. Sharma, M.; Nguyen, L.; Kuber, S.; Baradi, D. Testing IEC-61850 Sampled values-based transformer differential protection scheme. In Proceedings of the 74th Conference for Protective Relay Engineers (CPRE), Virtual Format, 22–25 March 2021; pp. 1–8. [CrossRef]
9. Ameli, A.; Ghafouri, M.; Zeineldin, H.H.; Salama, M.M.A.; El-Saadany, E.F. Accurate fault diagnosis in transformers using an auxiliary current-compensation-based framework for differential relays. *IEEE Trans. Instrum. Meas.* **2021**, *70*, 1–14. [CrossRef]

10. Bhalja, H.S.; Bhalja, B.R.; Agarwal, P. Rate of rise of differential current based protection of power transformer. In Proceedings of the IEEE 16th India Council International Conference (INDICON) 2019, Rajkot, India, 13–15 December 2019; pp. 1–4. [CrossRef]
11. Saleh, S.A.; Ozkop, E. ANSI 87T-based differential protection of 3ϕ solid-state transformers. In Proceedings of the IEEE Industry Applications Society Annual Meeting 2020, Detroit, MI, USA, 10–16 October 2020; pp. 1–9. [CrossRef]
12. Bahari, S.; Hasani, T.; Sevedi, H. A new stabilizing method of differential protection against current transformer saturation using current derivatives. In Proceedings of the 14th International Conference on Protection and Automation of Power Systems (IPAPS) 2019, Tehran, Iran, 31 December 2019–1 January 2020; pp. 33–38. [CrossRef]
13. Jafarian, P.; Agheli, A. Improvement of security of transformer differential protection in breaker-and-a-half substations. In Proceedings of the 14th International Conference on Protection and Automation of Power Systems (IPAPS) 2019, Tehran, Iran, 31 December 2019–1 January 2020; pp. 1–6. [CrossRef]
14. Andreev, M. Study of the impact of processes in electric power systems with RES on the operation of numerical differential transformer protection. In Proceedings of the IEEE PES Innovative Smart Grid Technologies Europe 2020, Delft, The Netherlands, 26–28 October 2020; pp. 354–358. [CrossRef]
15. Sherwani, A.; Kirçay, A. Improving the characteristic of percentage differential relay of power transformer using rogowski coil with extended park's vector approach. In Proceedings of the International Congress on Human-Computer Interaction, Optimization and Robotic Applications (HORA), Ankara, Turkey, 26–28 June 2020; pp. 1–7. [CrossRef]
16. ABB-Hitachi Energy, RET670: Transformer Protection IED, Application Manual. Available online: https://library.e.abb.com/public/d7aebf979c5f71d4c1257d930037406c/1MRK504138-UUS_-_en_Application_manual__Transformer_protection_RET670_2.0__ANSI.pdf (accessed on 15 July 2022).
17. ABB-Hitachi Energy, PCM600: Protection and Control IED Manager, Software. Available online: https://new.abb.com/medium-voltage/digital-substations/software-products/protection-and-control-ied-manager-pcm600 (accessed on 16 July 2022).
18. Kumar, S.; Kumar, D. An efficient hybrid approach for performance analysis of transformer protected. In Proceedings of the IEEE International Conference on Recent Trends in Electronics, Information & Communication Technology (RTEICT), Bangalore, India, 18–19 May 2018; pp. 754–758. [CrossRef]
19. Bonetti, A.; Gajic, Z. A new transformer differential protection approach on the basis of space-vectors examination. *Electr. Eng.* **2005**, *87*, 129–135. [CrossRef]
20. Gajic, Z.; Bonetti, A. Easy method for testing transformer differential relays. *Actual Trends Dev. Power Syst. Prot. Autom. Mosc.* **2009**, *142*, 386–392. Available online: https://www.researchgate.net/publication/330752719 (accessed on 27 June 2022).
21. Bejmert, D.; Kereit, M.; Mieske, F.; Rebizant, W.; Solak, K.; Wiszniewski, A. Power transformer differential protection with integral approach. *Int. J. Electr. Power Energy Syst.* **2020**, *118*, 105859. [CrossRef]
22. Tripathy, M. Power transformer differential protection based on neural network principal component analysis, harmonic restraint and Park's plots. *Adv. Artif. Intell.* **2012**, *2012*, 1–10. [CrossRef]
23. Villamagna, N.; Crossley, P.A. A CT saturation detection algorithm using symmetrical components for current differential protection. *IEEE Trans. Power Deliv.* **2007**, *21*, 38–45. [CrossRef]
24. Samet, H.; Shadaei, M.; Tajdinian, M. Statistical discrimination index founded on rate of change of phase angle for immunization of transformer differential protection against inrush current. *Int. J. Electr. Power Energy Syst.* **2022**, *134*, 0142–0615. [CrossRef]
25. Bkhaitawi, A.H.Z.; Abdoos, A.A.; Ebadi, A. An adaptive restraint method to improve performance of ground differential protection of power transformer. *Int. J. Eng. IJE Trans. B Appl.* **2022**, *35*, 2213–2219. [CrossRef]
26. Darwish, H.A.; Lehtonen, M. Current differential relay with a power-current spectrum blocking for transformer protection. In Proceedings of the IEEE Buchar. PowerTech 2009, Bucharest, Romania, 28 June–2 July 2009; pp. 1–7. [CrossRef]
27. Desai, J.P.; Makwana, V.H. Modeling and implementation of percentage bias differential relay with dual-slope characteristic. In Proceedings of the IEEE Texas Power and Energy Conference (TPEC), College Station, TX, USA, 2–5 February 2021; pp. 1–6. [CrossRef]
28. Rashid, M.; Raheem, A.; Shakoor, R.; Arfeen, Z.A.; Husain, N. SCADA based differential protection of power transformers. In Proceedings of the 6th International Multi-Topic ICT Conference (IMTIC), Jamshoro & Karachi, Pakistan, 10–12 November 2021; pp. 1–5. [CrossRef]
29. Ehsan, U.; Jawad, M.; Javed, U.; Shabih, Z.K.; Ur Rehman, A.; Rassolkin, A.; Althobaiti, M.M.; Hamam, H.; Shafiq, M.A. Detailed testing procedure of numerical differential protection relay for EHV auto transformer. *Energies* **2021**, *14*, 8447. [CrossRef]
30. Sevov, L.; Zhang, Z.; Voloh, I.; Cardenas, J. Differential protection for power transformers with non-standard phase shifts. In Proceedings of the 64th Annual Conference for Protective Relay Engineers, College Station, TX, USA, 11–14 April 2011; pp. 301–309. [CrossRef]
31. Shah, A.M.; Bhalja, B.R.; Patel, R.M. Power transformer differential protection using S-transform and Support Vector Machine. In Proceedings of the 2016 National Power Systems Conference (NPSC), Bhubaneswar, India, 19–21 December 2016; pp. 1–6. [CrossRef]
32. Ahmadzadeh-Shooshtari, B.; Rezaei-Zare, A. Advanced transformer differential protection under GIC Conditions. *IEEE Trans. Power Deliv.* **2022**, *37*, 1433–1444. [CrossRef]
33. Rocha, D.C.G.; Batista, W.H.; Coelho, A.L.M.; Marcos, R.A. Practical approach to testing the transformer differential protection for internal and external faults, CT saturation and inrush transients. In Proceedings of the 14th International Conference on Developments in Power System Protection, The Institution of Engineering and Technology (IET), Belfast, UK, 12–15 March 2018; pp. 2051–3305. [CrossRef]